ELSEVIER

International Journal of Heat and Fluid Flow 22 (2001) 372–379

International Journal of HEAT AND FLUID FLOW

www.elsevier.com/locate/ijhff

Super-mixing combustion enhanced by resonance between micro-shear layer and acoustic excitation

H. Yoshida [a,*], M. Koda [b], Y. Ooishi [c], K.P. Kobayashi [d], M. Saito [a]

[a] *Department of Mechanical Engineering, Kyoto University, Yoshida-honmachi, Sakyo-ku, Kyoto 606-8501, Japan*
[b] *Department of Mechanical Engineering and Science, Tokyo Institute of Technology, O-okayama, Meguro-ku, Tokyo 152-8552, Japan*
[c] *Power Systems and Services Company, Toshiba Corporation, Suehirocho, Tsurumi-ku, Yokohama 230-0045, Japan*
[d] *Department of Mechanical Engineering, Meiji University, Higashi-mita, Tama-ku, Kawasaki 214-8571, Japan*

Abstract

In terms of the application of high-speed and high-load combustion to isothermal-expansion combustion proposed by the authors, flow and reaction control of relatively small diffusion flames ejected from nozzles 0.5 and 1 mm in width are investigated using acoustic resonance; this study is the first step for the mixing control of a micro-diffusion flame which is considered to be a final goal of the relevant studies. In nonreacting jet experiments, Schlieren visualization and flow measurement by a hot-wire anemometer show that marked amplification of turbulence is induced by acoustic excitation with frequencies proportional to the nozzle-exit velocity. Analogously, visual observation, temperature and measurements of concentration for the reacting jet demonstrate that combustion is significantly enhanced under the resonant condition.

Keywords: Diffusion combustion; Resonance mixing; Micro-shear layer; Acoustic excitation

1. Introduction

Microflames, the length scale of which is on the order of 100 μm, have significant potential for high-speed and high-load combustion. Furthermore, we can also expect high controllability, because the micro-shear layers of such flames are very sensitive to small external perturbations.

One probable application of microflames is the extremely high-speed combustion in an *isothermal-expansion* nozzle: the concept of *isothermal-expansion combustion* was proposed by Echigo et al. (1999) and Saito et al. (1999) from the viewpoint of energy-regenerating combustion (Echigo, 1996). In the context of isothermal-expansion combustion, the decrease in temperature due to acceleration through the nozzle should be compensated for by rapid combustion of additional fuel injected into the nozzle passage, and the resulting increase in the kinetic energy of the flowing gas is favorable in terms of the effective energy conversion. To realize this novel combustion system, combustion enhancement based on intense mixing of fuel and air is indispensable.

A number of studies have been reported which deal with the active control of free jets with or without reaction (Gad-el-Hak, 2000; Chao and Jeng, 1992; Gutmark et al., 1996; Seol and Goldstein, 1998; Carlton et al., 1999). To the authors' knowledge, however, its application to microflames has never been evaluated. Therefore, in this study, as the first step for the mixing control of a micro-diffusion flame, relatively small diffusion flames ejected from nozzles 0.5 and 1 mm in width are investigated. Although this size is still 10 times as great as that of the authors' original concept, no measurement technique for such micro-scale experiments was available to the authors. As an active control technique, acoustic resonance is applied, because mechanical control methods are not easily applicable to such phenomena with relatively high characteristic frequency.

2. Experimental apparatus and technique

2.1. Experimental setup

Fig. 1 shows a schematic diagram of the experimental setup. Planar (aspect ratio 10:1) nozzles 0.5 and 1 mm in width were used. Because of the spatial resolution of measurement, however, we obtained detailed data only for the nozzle of 1 mm in width. The nozzles had a contraction ratio of 21:1 to ensure a uniform exit velocity profile.

The center of the exit port of the nozzle is taken as the origin of the coordinate system; x and y denote distances parallel to and normal to the jet, respectively, and B denotes the nozzle width. In order to apply acoustic excitation, a speaker of 120 mm in diameter was set as shown Fig. 1. The speaker was driven by a sinusoidal wave input, and its output power was fixed at 112 dB irrespective of the frequency.

* Corresponding author.
E-mail address: yoshida@mech.kyoto-u.ac.jp (H. Yoshida).

0142-727X/01/$ - see front matter
PII: S0142-727X(01)00103-5

Notation

B	nozzle width
f_r	resonance frequency
Re	Reynolds number, $Re = U_0B/v$
St	Strouhal number, $St = f_rB/U_0$
U	mean velocity in x direction
U_0	mean velocity in x direction at nozzle exit
u_{rms}	root-mean-square of fluctuating velocity in x direction
x	streamwise coordinate
y	normal coordinate

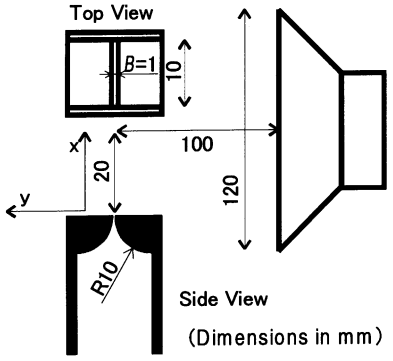

Fig. 1. Schematic diagram of experimental setup.

2.2. Nonreacting jet measurement

Prior to the combustion experiments, we conducted nonreacting jet measurements, in which carbon dioxide was injected into the surrounding air; this was because the Schlieren technique was available for flow visualization based on the density difference between carbon dioxide and air. A high-speed video camera with a recording rate of 9000 images per second was used for visual observation.

Although the flow velocity was measured using a hot-wire anemometer, the data obtained should be interpreted qualitatively, because the test fluid was a mixture of carbon dioxide and air, whereas the hot-wire anemometer was calibrated using air flow.

2.3. Reacting jet measurement

For the combustion experiment, methane was used as the fuel injected from the nozzle. Flame shapes with and without the Schlieren technique were observed using the high-speed video camera. Since the dependence of the flame shape on the acoustic frequency was so remarkable, the resonance condition could be accurately determined by visual observation without velocity measurement.

Gas temperature was measured using a thermocouple with a 0.2 mm bead diameter, and the concentrations of major species were measured using a gas chromatograph with a sampling probe 0.6 mm in diameter.

3. Results and discussion

3.1. Nonreacting jet

3.1.1. Frequency dependence and resonance frequency

In order to clearly show the effect of the acoustic excitation on the jet mixing, we first discuss the data obtained

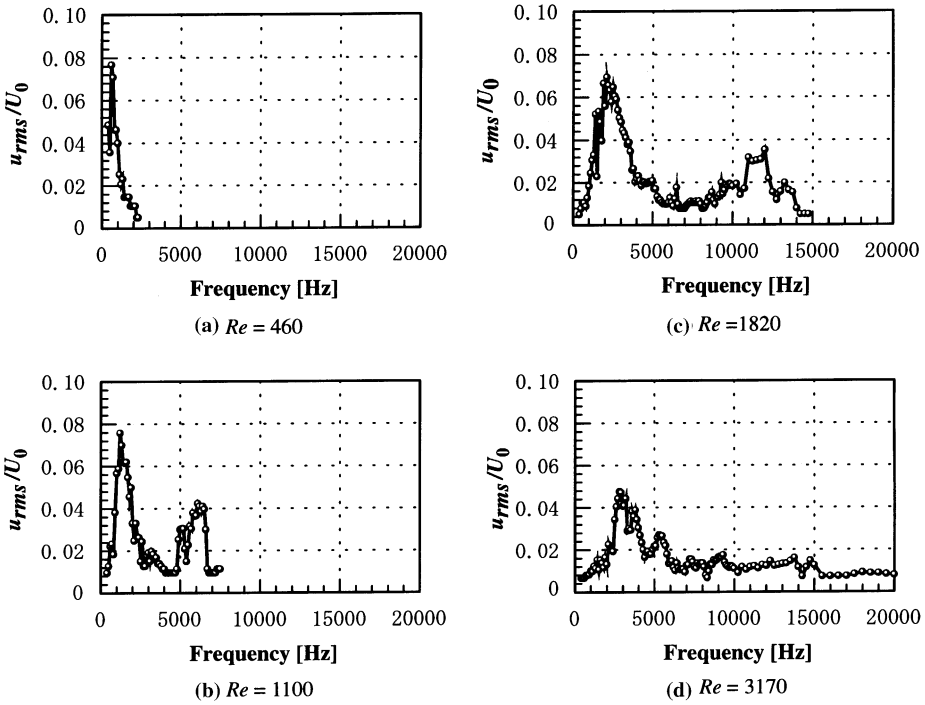

Fig. 2. Variation of turbulent intensity with applied frequency ($x/B = 6$ and $y/B = 0$).

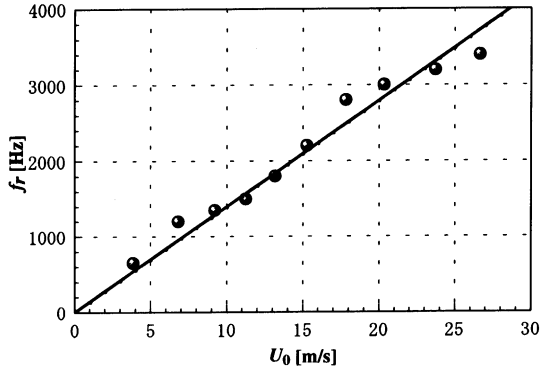

Fig. 3. Relationship between resonance frequency and exit velocity from the nozzle.

using the hot-wire anemometer. Fig. 2 shows the relationship between the frequency of the applied excitation and the resulting turbulent intensity u_{rms}/U_0 at $x/B = 6$ and $y/B = 0$, where U_0 is the exit velocity from the nozzle. In the present experiment, the Reynolds number based on U_0 and B is relatively low ($460 \sim 3170$); hence, without acoustic excitation, the turbulent intensity u_{rms}/U_0 at $x/B = 6$ and $y/B = 0$ is less than 0.01. When the acoustic excitation is applied, however, the turbulent intensity changes markedly depending on the frequency. Although two peaks are shown in Figs. 2(b)–(d), in the present study, attention is focused on the highest peak, which is referred to as the resonance frequency f_r.

From the data presented in Fig. 3, the resonance frequency f_r is found to be proportional to the exit velocity from the

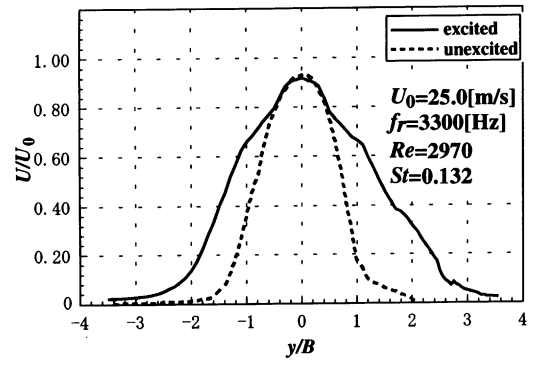

(c) $x/B = 6$

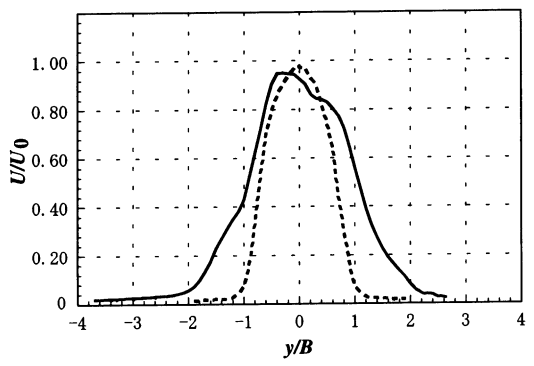

(b) $x/B = 4$

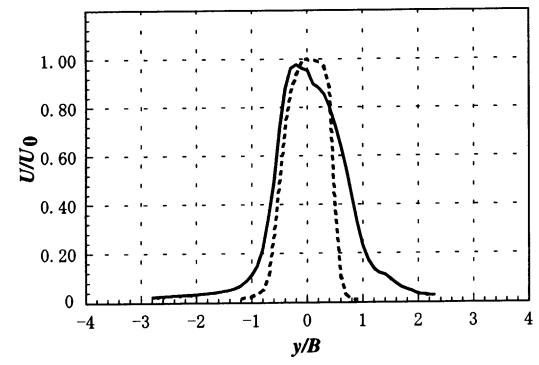

(a) $x/B = 2$

Fig. 4. Time-mean velocity for $Re = 2970$ and $f_r = 3300$ Hz.

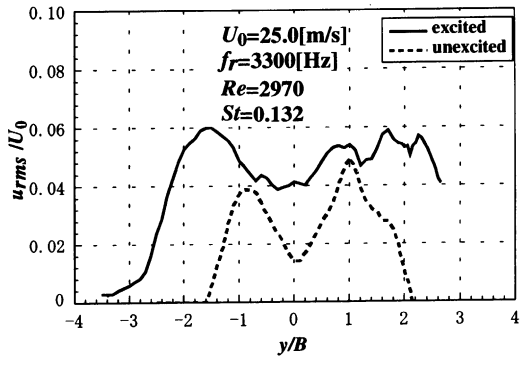

(c) $x/B = 6$

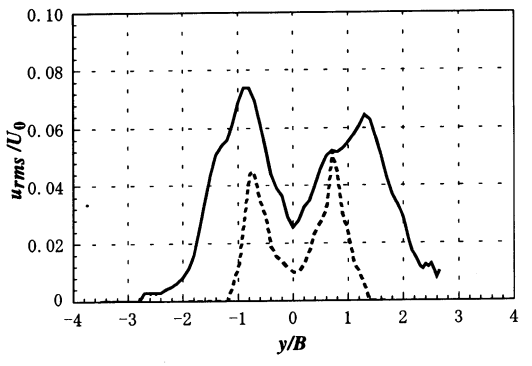

(b) $x/B = 4$

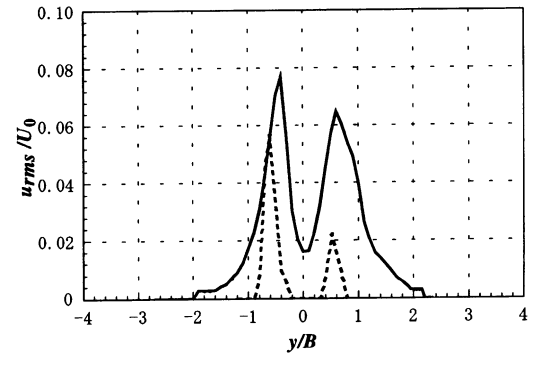

(a) $x/B = 2$

Fig. 5. Turbulent intensity for $Re = 2970$ and $f_r = 3300$ Hz.

nozzle U_0, thus the Strouhal number $St = f_r B/U_0$ is nearly constant, i.e., $St \sim 0.15$.

Note that, although the turbulent intensity discussed here was measured at the centerline inside or just outside the potential core of the jet, we confirmed that every region of the entire flowfield strongly correlates with each other from the observation based on the high-speed video images.

3.1.2. Mixing characteristics under resonant condition

Figs. 4 and 5 show the distributions of the time-mean velocity U and the turbulent intensity u_{rms}/U_0 at $x/B = 2, 4$, and 6 with $Re = 2970$ (the exit velocity from the nozzle $U_0 = 25.0$ m/s) and the frequency of the applied acoustic excitation $f_r = 3300$ Hz. Upon acoustic excitation both distributions become much broader than those of the unexcited case.

Fig. 6 compares typical Schlieren photographs of the resonant conditions. Although a high-speed video was used, the images are not so clear as a result of high magnification and relatively high velocities of the flow. However, the transition from laminar to turbulent states is found to be markedly enhanced by acoustic excitation; a neck associated with the sudden change of the spreading angle of the jets is also seen in Fig 6.

3.2. Reacting jet

3.2.1. Visual observation

Since the present diffusion flames were clearly visible, the resonant condition was specified by continuously changing the frequency of the acoustic excitation. Table 1 lists the conditions corresponding to the photographs shown in Figs. 7 and 8. Although the Strouhal number is also constant for the reacting jet, its value is about half of that for the nonreacting jet. In the following, the data for $Re = 1410$ are omitted because qualitatively they are almost similar to those for $Re = 920$.

The photographs of the reacting jet are shown in Figs. 7 and 8, respectively; note that in Fig. 7, a relatively wide area ($x/B < 700$) is included, unlike in Figs. 6 or 8. In Fig. 7, the flame with acoustic excitation is much wider and shorter than the unexcited one. Furthermore, clearly seen from real-time observations, the flame oscillation is significantly amplified by acoustic excitation. Qualitatively this corresponds to the intense mixing demonstrated in the nonreacting jet experiment.

However, the flame behavior changes markedly depending on the Reynolds number. Compared with the case of $Re = 580$, the case of $Re = 920$ (also of $Re = 1410$, which is omitted here) shows intense oscillation behavior. This behavior is also confirmed from the temperature measurement later in Fig. 9(b). To investigate the detail of this point, we observed the Schlieren photographs focused on the region near the nozzle exit. In Fig. 8, the outer boundaries correspond to the flame sheet, while the inner almost straight lines correspond to the edge of cold fuel flow injected from the nozzle. If acoustic excitation is not applied, for both cases of $Re = 580$ and $Re = 920$, a laminar-diffusion flame is formed from the nozzle exit. On the other hand, for the case of $Re = 580$ with acoustic resonance, there appears a neck of the flame sheet at $x/B = 15$. This neck is basically considered to be the counterpart to that found in Fig. 6 for the nonreacting jet. With increasing Reynolds number, a flame attached to the nozzle exit becomes thin, and finally the lifted flame is formed. In other words, the above-mentioned neck shifts to the upstream direction with increasing flow velocity, and simultaneously the flame attached

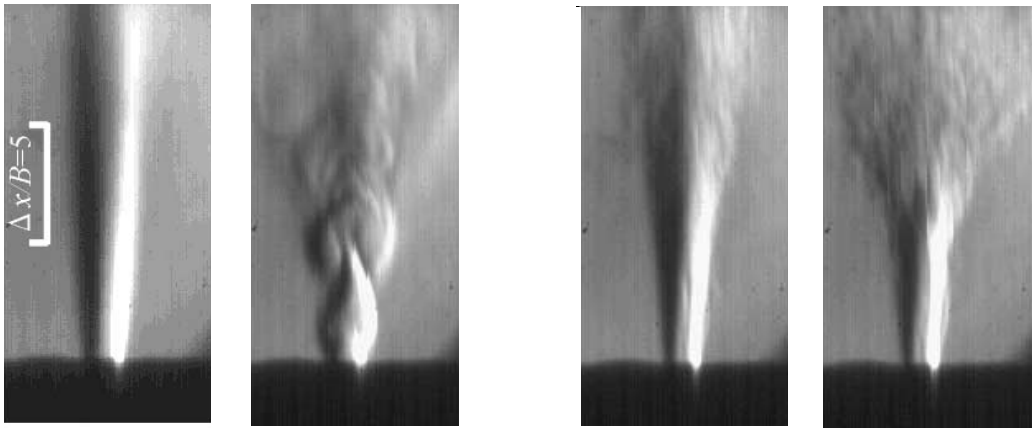

Fig. 6. Schlieren photographs under the resonant conditions.

Table 1
Resonant condition

Exit velocity from the nozzle U_0 (m/s)	Reynolds number $Re = U_0 B/\nu$	Resonance frequency f_r (Hz)	Strouhal number $St = f_r B/U_0$
10.1	580	900	0.089
16.0	920	1350	0.084
24.4	1410	2200	0.090

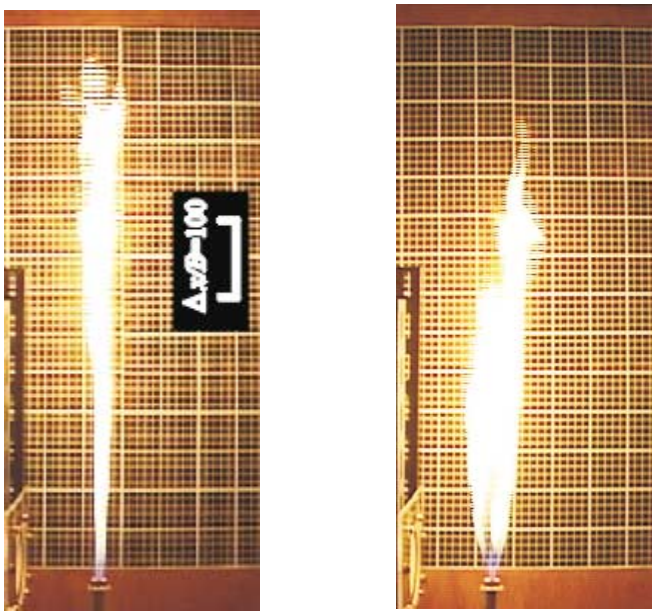

without excitation resonance

(a) $Re = 580$

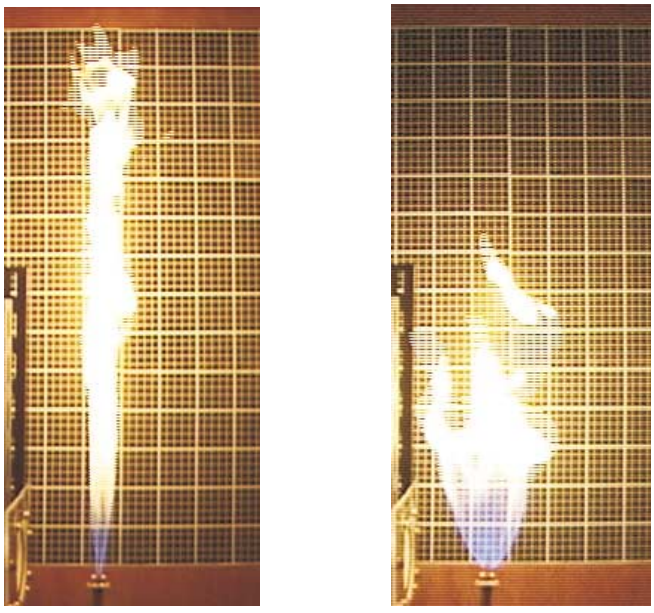

without excitation resonance

(b) $Re = 920$

Fig. 7. Photographs of the reacting jet under resonant conditions.

to the nozzle exit disappears. For the case of $Re = 920$, the neck locates at $x/B = 4$; once the flame is lifted, the flame intensely oscillates around the neck which is not so tightly fixed at $x/B = 4$. For the case of $Re = 1410$ (not shown here), the flame is also stabilized at $x/B = 4$ by acoustic excitation, whereas the unexcited flame lifts to $x/B = 35$. In the cases of $Re = 920$ and $Re = 1410$ with acoustic excitation, the envelop of the flame sheet formed near the neck is extremely wider than the nozzle width, which is attributed to the relatively small scale of the present flame. Although the behavior of the lifted flame under acoustic excitation is discussed by Chao and Jeng (1992), a simple extension of their findings to the present case is difficult because of the large difference between the characteristic length scales for two experiments.

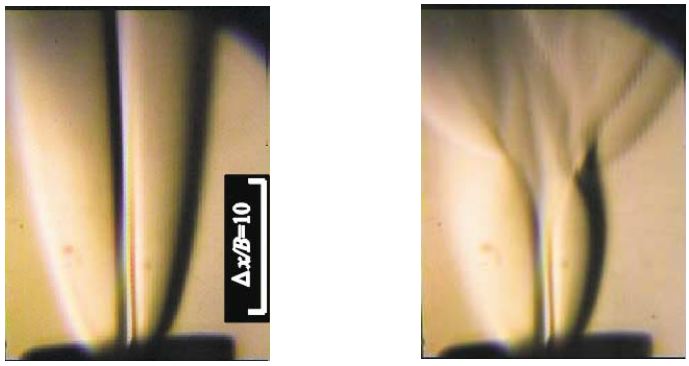

Fig. 8. Schlieren photographs of the reacting jet under resonant conditions.

3.2.2. Temperature measurement

Fig. 9 shows the time-mean temperature distribution measured at $x/B = 0$, 10, 20, and 30. The color map is obtained by interpolating the data measured at the four values of x/B. The enhancement of mixing is also confirmed from the temperature field. In particular, the width of the combustion region at $x/B = 30$ for $Re = 920$ is more than four times as wide as that without excitation. This corresponds to the fact described in detail in Section 3.1.1. The decrease in the maximum temperature is mainly attributed to the intense lateral oscillation of the mixing region.

3.2.3. Concentration measurement

Fig. 10 shows the molar fractions of major species on the centerline ($y/B = 0$) detected by gas chromatography. In all cases, the molar fraction of CH_4 decreases, while that of N_2 increases. Although the overall distributions of the concentrations of the species have not yet been obtained, the tendencies found at the jet centerline indicate that the combustion reaction is also effectively enhanced by the acoustic resonance.

4. Conclusions

To gain a basic understanding on the controllability of microflames, acoustic excitation was applied to the planar jets injected from the nozzles 0.5–1 mm in width. The phenomena were observed from various aspects; measurements for velocity, temperature, and concentrations of various species were conducted as well as flow visualization.

In both the nonreacting and reacting jets, resonant phenomena were clearly confirmed. At the resonant conditions, the transition from laminar to turbulent flow is enhanced, and consequently the turbulent intensity of the flow increases markedly. The Strouhal number for the resonant condition is almost constant for each case, but varies widely depending on reacting or nonreacting conditions.

The diffusion combustion at the resonant condition was very different from that without excitation. In addition to the above-mentioned changes, the flame stability is greatly influenced depending on the Reynolds number. Once the flame is not so tightly fixed or stabilized at the downstream location of the nozzle exit, the flame oscillation is significantly enhanced by acoustic oscillation, and the flame becomes much wider and shorter than that without excitation.

The experiment conducted in the present study is smaller compared with those in the previous relevant studies. However, it is still one order of magnitude larger than those the authors aimed at. Since the relating phenomena are essentially nonlinear, the second-step study for smaller size is also required with the aid of novel and sophisticated measurement technique.

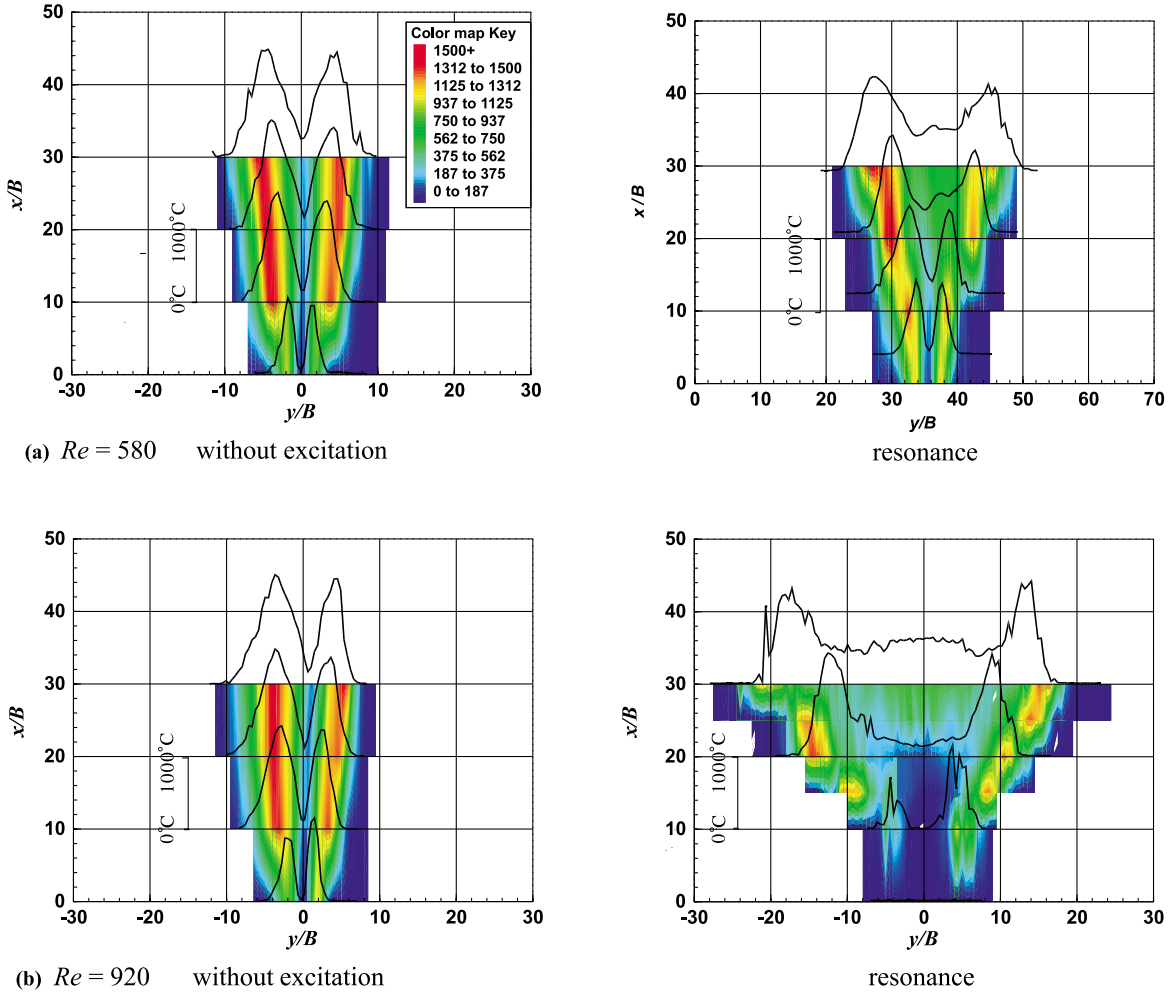

Fig. 9. Mean temperature distribution.

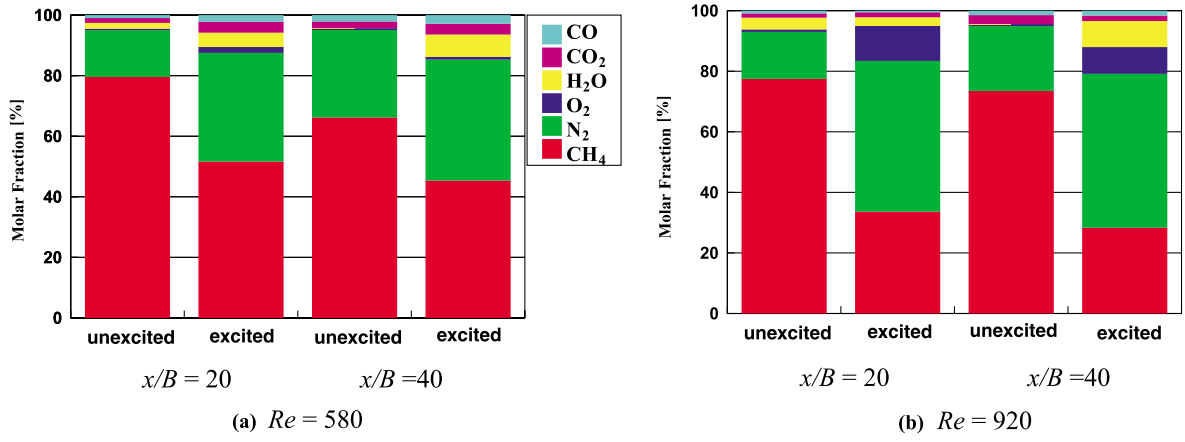

Fig. 10. Molar fraction of major species.

Acknowledgements

This work was supported in part by the Ministry of Education, Science, Sports and Culture through a Grant-in-Aid for Scientific Research (C), No. 10650202.

References

Carlton, J.D., Hertzberg, J.R., Foerster, K., Linne, M.A., 1999. Side jet formation and split flames. Turbulence and Shear flow Phenomena – 1, Begell House, New York, pp. 207–212.

Chao, Y.-C., Jeng, M.-S., 1992. Behavior of the lifted jet flame under acoustic excitation. In: Twenty-Fourth Symposium (International) on Combustion, pp. 333–340.

Echigo, R., 1996. Energy regenerating combustion for advanced energy conversion. In: Proceedings of the Third KSME–JSME Thermal Engineering Conference, III, pp. 1–8.

Echigo, R., Saito, M., Yoshida, H., Kobayashi. K.P., 1999. Isothemal-expansion combustion aiming at effective regeneration of energy – I. A concept of a new combustion system and its energy/energy analyses. In: Proceedings of the Fifth ASME/JSME Joint Thermal Engineering Conference, AJTE 99-6334.

Gad-el-Hak, M., 2000. Flow Control Passive, Active, and Reactive Flow Management. Cambridge University Press, Cambridge.

Gutmark, E.J., Parr, T.P., Wilson, K.J., Schadow, K.C., 1996. Applications of active combustion control via synchronized fuel injection into vortices. Transport Phenomena in Combustion 2, 1634–1645.

Saito, M., Yoshida, H., Kobayashi, K.P., Echigo, R. 1999. Isothemal-expansion combustion aiming at effective regeneration of energy – II. A one-dimensional analysis with control of streamwise variation in cross-sectional area. In: Proceedings of the Fifth ASME/JSME Joint Thermal Engineering Conference, AJTE 99-6335.

Seol, W.S., Goldstein, R.J., 1998. Visualization of the effect of acoustic excitation on vortex structure and energy separation in jets. In: Proceedings of the 11th International Heat Transfer Conference, vol. 5, pp. 491–496.